HHS Public Access

Author manuscript

Oncogene. Author manuscript; available in PMC 2016 June 04.

Published in final edited form as:

Oncogene. 2015 June 4; 34(23): 2958–2967. doi:10.1038/onc.2014.245.

GD3 Synthase regulates epithelial-mesenchymal transition and metastasis in breast cancer

Tapasree Roy Sarkar[1], **Venkata L Battula**[7], **Steven J Werden**[1], **Geraldine V Vijay**[1], **Esmeralda Q Ramirez-Peña**[1], **Joseph H Taube**[1], **Jeffrey T Chang**[4], **Naoyuki Miura**[5], **Weston Porter**[6], **Nathalie Sphyris**[1], **Michael Andreeff**[7,*], and **Sendurai A Mani**[1,2,3,*]

[1]Departments of Translational Molecular Pathology, University of Texas Health Science Center at Houston, Houston, Texas

[3]Metastasis Research Center, University of Texas Health Science Center at Houston, Houston, Texas

[3]Center for Stem Cells and Developmental Biology, University of Texas Health Science Center at Houston, Houston, Texas

[4]Department of Integrative Biology and Pharmacology, University of Texas Health Science Center at Houston, Houston, Texas

[5]Department of Biochemistry, Hamamatsu University School of Medicine, Hamamatsu, Japan

[6]Department of Veterinary Integrative Biosciences, Texas A & M University

[7]Department of Leukemia, University of Texas MD Anderson Cancer Center

Abstract

The epithelial-mesenchymal transition (EMT) bestows cancer cells with increased stem cell properties and metastatic potential. To date, multiple extracellular stimuli and transcription factors have been shown to regulate EMT. Many of them are not druggable and therefore it is necessary to identify targets, which can be inhibited using small molecules to prevent metastasis. Recently, we identified the ganglioside GD2 as a novel breast cancer stem cell marker. Moreover, we found that GD3 synthase (GD3S)—an enzyme involved in GD2 biosynthesis—is critical for GD2 production and could serve as a potential druggable target for inhibiting tumor initiation and metastasis. Indeed, there is a small-molecule known as triptolide that has been shown to inhibit GD3S function. Accordingly, in this manuscript, we demonstrate that the inhibition of GD3S using shRNA or triptolide compromises the initiation and maintenance of EMT instigated by various signaling pathways, including Snail, Twist and TGF-β1 as well as the mesenchymal characteristics of claudin-low breast cancer cell lines (SUM159 and MDA-MB-231). Moreover, GD3S is necessary for wound healing, migration, invasion and stem cell properties *in vitro*. Most importantly, inhibition of GD3S *in vivo* prevents metastasis in experimental as well as in

[*]**Corresponding Authors:** Michael Andreeff, Department of Leukemia, The University of Texas MD Anderson Cancer Center, Houston, TX 77030. Phone: 713-792-9638; Fax: 713-834-6082; mandreef@mdanderson.org, Sendurai A. Mani, Department of Translational Molecular Pathology, Metastasis Research Center, The University of Texas MD Anderson Cancer Center, Houston, TX 77030. smani@mdanderson.org.

CONFLICT OF INTEREST

The authors are inventors of a patent application based on the work described here.

spontaneous syngeneic wild-type mouse models. We also demonstrate that the transcription factor FOXC2, a central downstream mediator/effector of several EMT pathways, directly regulates GD3S expression by binding to its promoter. In clinical specimens, the expression of GD3S correlates with poor prognosis in triple negative human breast tumors. Moreover, GD3S expression correlates with activation of the c-Met signaling pathway leading to increased stem cell properties and metastatic competence. Collectively, these findings suggest that the GD3S-c-Met axis could serve as an effective target for the treatment of metastatic breast cancers.

Keywords

GD3S; EMT; c-Met; metastasis; NF-kB; FOXC2

INTRODUCTION

The epithelial-mesenchymal transition (EMT) is a normal developmental process where by epithelial cells lose their epithelial characteristics, such as cell-cell adhesions, and undergo a dramatic remodeling of the cytoskeleton that culminates in the acquisition of a motile mesenchymal phenotype.(1–3) This complex series of morphological changes is accompanied by the downregulation of epithelial markers (e.g., E-cadherin) and the upregulation of mesenchymal markers (e.g., N-cadherin and vimentin). EMT occurs during embryogenesis as well as in tissue repair, fibrosis, and cancer.(4–6) During cancer progression, the EMT process endows cancer cells with the ability to metastasize. EMT and metastasis are regulated by distinct signaling molecules present in the tumor microenvironment (e.g., transforming growth factor-β1 (TGF-β1), Wnt, tumor necrosis factor-α (TNF-α), hepatocyte growth factor (HGF), and Notch),(7–9) and a variety of intracellular transcription factors (e.g., Snail, Twist, and Goosecoid).(10–16

Cells that undergo EMT also acquire self-renewal capabilities, express stem cell-associated $CD44^{high}CD24^{low}$ cell-surface markers, and become resistant to chemotherapy.(17–22) We recently found that epithelial cells induced to undergo EMT behave similar to mesenchymal stem/stromal cells (MSCs).(23) Furthermore, the ganglioside GD2, normally known to be expressed in MSCs, is also expressed on the cell surface of breast CSCs and can be used for their isolation.(24) Although suppression of GD3 synthase (GD3S), the rate-limiting enzyme for GD2 biosynthesis, hampers mammosphere formation and stem cell properties,(24) its role in metastasis is not known. Among various signaling pathways, c-Met (HGF receptor) is frequently deregulated in many cancers, and is known to promote invasion, survival, and metastasis.(25–33) Moreover, GD3S expression has been shown to enhance the proliferation of MDA-MB-231 cells through the activation of c-Met.(34) In this manuscript, we describe that GD3S not only regulates EMT and CSC properties, but also metastasis *in vivo*. GD3S regulates stem cell function via c-Met and the expression of GD3S is regulated by FOXC2, a transcription factor functioning downstream of several EMT signaling pathways. In addition, we report that GD3S expression is high in EMT/CSC-enriched claudin-low/triple negative human breast cancers and that its expression correlates with poor patient survival.

RESULTS

GD3S is necessary for the initiation and maintenance of EMT

Earlier, we found that the ganglioside GD2 serves as a marker for breast CSCs and that the enzyme GD3S is essential for GD2 biosynthesis.(24) Since CSCs and cells that have undergone EMT share many properties, we investigated whether GD3S is necessary for maintaining the mesenchymal status of cells experimentally induced to undergo EMT (HMLE-Snail, HMLE-Twist) as well as established breast cancer cell lines (SUM159, MDA-MB-231). For this, we used shRNA to suppress GD3S expression and found that inhibition of GD3S expression substantially altered the morphology of each cell type, causing increased clustering of cells into epithelial-like islands with the establishment of cell-cell contacts and reduced fibroblastic morphology (Figure 1a). Furthermore, the expression of the mesenchymal markers N-cadherin, fibronectin and vimentin were reduced to varying degrees in the absence of GD3S (Figure 1b).

Likewise, the inhibition of GD3S activity in the aforementioned cells using the small molecule inhibitor triptolide(35) induced an epithelial-like morphology (Figure 1c) accompanied by a reduction in the expression of mesenchymal markers (Supplementary Figure 1a) without changing the rate of cell proliferation (Supplementary Figure 1b). In addition, we observed increased expression of the epithelial marker E-cadherin in HMLE-Snail, HMLE-Twist, and MDA-MB-231 cells, but not in SUM159 cells (Figure 1b and Supplementary Figure 1a). Collectively, these findings suggest that GD3S is necessary for the maintenance of mesenchymal properties of both cells induced to undergo EMT as well as mesenchymal-appearing breast cancer cell lines.

Since the induction of EMT in tumors can generate new CSCs and/or replenish the existing CSC pool, deterring the mechanisms underlying the initiation of EMT is as important as targeting cells that have already undergone EMT. To examine the potential role of GD3S in the initiation of EMT, we utilized a TGF-β1 inducible model and report that blocking GD3S activity prevented the acquisition of a spindle-like morphology in TGFβ-treated (2 ng/ml) MCF10A cells (Figures 1d, e and Supplementary Figure 1c). We observed similar results using the mouse mammary EpH4Ras epithelial cell line (Supplementary Figure 1d), further supporting the notion that GD3S is necessary for TGF-β1 mediated induction of EMT. In the same manner, we found that the Snail-ER fusion protein, known to elicit EMT in the presence of 4-OHT,(19) failed to confer an overt mesenchymal morphology, when GD3S expression was suppressed using shRNA (Figures 1f and g) or triptolide (Figures 1h and i). Accordingly, the induction of mesenchymal markers was delayed in these cells compared to control counterparts (Figures 1g, i). GD3S expression is high in cells that have undergone EMT as well as in triple negative breast cancer (TNBC) cells when compared to cells with no EMT features (Supplementary Figure 1e) which further underscores the links between GD3S and EMT properties. Collectively, these findings show that GD3S plays a critical role in the maintenance of a mesenchymal phenotype in cells that have undergone EMT, as well as in the initiation of EMT in response to Snail, Twist, and TGF-β1 in several model systems.

GD3S regulates invasion and motility of cancer cells

Passage of cells through an EMT not only promotes the acquisition of stem cell properties but is also known to confer concomitant migratory and invasive capabilities.(1–3) To test whether GD3S also regulates invasion, HMLE-Snail and MDA-MB-231 cells were cultured in a 3D laminin-rich extracellular matrix Matrigel (3D lrECM). As expected, vehicle-treated cells grew as highly invasive stellate structures (Figure 2a). In sharp contrast, when we inhibited GD3S expression using triptolide, cells formed non-invasive multicellular structures (Figure 2a) with the basement membrane intact as indicated by the presence of a continuous laminin V layer (Figure 2b). Moreover, the number of invasive acinus structures was significantly decreased in triptolide-treated lrECM cultures (Figure 2c). Similar results were obtained using MDA-MB-231 and HMLE-Snail cells expressing GD3S shRNA (Figures 2d and e). We also employed MCF10A cells known to form highly organized multicellular acini with an intact basement membrane(36) when cultured in 3D lrECM. However, in the presence of TGF-β1, MCF10A cells form irregular invasive structures with a disrupted basement membrane. We found that concurrent exposure to triptolide considerably decreased TGF-β1 mediated invasive acinus formation and restored the integrity of the basement membrane when compared to vehicle-treated cells (Figure 2f). Finally, we also investigated the role of GD3S in cell migration using a scratch assay and found that inhibition of GD3S expression by triptolide (Figure 2g) or shRNA-mediated silencing (Figure 2h) reduced migration significantly in MDA-MB-231 and HMLE-Snail cells. Collectively, these findings show that GD3S is necessary for EMT as well as EMT-associated cell migration and invasive properties.

GD3S plays an important role in metastasis

In order to examine the role of GD3S in the regulation of metastasis, we injected 4T1 cells (10,000) orthotopically into the mammary fat-pad of syngeneic wild type BALB/c mice. Once the mice had developed palpable tumors (Figure 3b), we treated one set with triptolide —which inhibits GD3S, mesenchymal markers (Figure 3a) as well as GD2 expression in 4T1 cells (Supplementary Figure 2a)—and the other set with vehicle. The vehicle-treated mice developed lung metastasis as evidenced by strong luminescence in the lungs, whereas the triptolide-treated mice had significantly decreased luminescence in the lungs (Figure 3c), indicating a reduced metastatic burden. To examine the role of GD3S in primary tumor formation and metastasis, we suppressed the expression of GD3S using shRNA in 4T1 cells. Upon confirming the knockdown (Supplementary Figure 2b), we injected 4T1 cells expressing control-shRNA or GD3S-shRNA (100,000) orthotopically into the mammary fat-pad of syngeneic wild type BALB/c mice. Remarkably, the GD3S-shRNA expressing 4T1 cells yielded primary tumors which were significantly smaller in size compared to those generated by control-shRNA 4T1 cells, with the exception of one mouse (Supplementary Figure 2c). In addition, mice harboring the control-shRNA expressing 4T1 cells developed large lung foci as evidenced by strong luminescence in the lungs, whereas the mice injected with GD3S-shRNA expressing 4T1 cells exhibited significantly reduced luminescence in the lungs, consistent with a markedly reduced metastatic burden (Supplementary Figure 2d). To confirm that the reduction in lung nodules in mice harboring GD3S-shRNA expressing 4T1 cells was not due to the reduction in primary tumor size, we investigated the role of GD3S in experimental metastasis. For this, we injected 0.5×10^6 RFP/luciferase-labeled MDA-

MB-231 cells via the tail vein and subsequently treated the mice with either vehicle or triptolide for six weeks and analyzed for the presence of lung metastases using bioluminescent imaging.(24, 35) Whereas mice harboring vehicle-treated or control shRNA expressing MDA-MB-231 cells developed metastases (Figures 3d, e), inhibition of GD3S using triptolide or shRNA significantly reduced the metastatic burden (Figures 3d, e).

Using hematoxylin and eosin (H & E) staining, we further confirmed the presence of large metastatic foci in the lungs of mice injected with control-shRNA expressing MDA-MB-231 cells (Figure 3f) but not in mice injected with GD3S-shRNA expressing MDA-MB-231 cells. Similarly, we only detected metastatic foci in the lungs of mice injected with MDA-MB-231 cells and subsequently treated with vehicle (Figure 3f) but not in mice injected with MDA-MB-231 cells and subsequently treated with triptolide. In order to distinguish whether GD3S regulates seeding of the cells to the lung or the expansion of seeded cells into macroscopic nodules, we performed immunofluorescence using anti-RFP on the lungs of mice injected with RFP-labeled MDA-MB-231 cells and treated with triptolide or RFP-labeled MDA-MB-231 cells expressing GD3S-shRNA relative to their respective control mice. While, we observed extensive RFP staining indicative of the presence of large metastatic foci in the lungs of mice injected with control-shRNA expressing MDA-MB-231 cells (Figure 3f, lower panel) or vehicle-treated MDA-MB-231 cells (Figure 3f, lower panel), we did not find colonies of RFP-positive cells in mice injected with GD3S-shRNA expressing MDA-MB-231 cells or in the triptolide-treated mice harboring MDA-MB-231 cells. However, we did observe numerous RFP-positive single cells in the lungs of mice harboring MDA-MB-231 cells expressing GD3S-shRNA or mice harboring MDA-MB-231 cells that were treated with triptolide, even though we did not observe lung nodules in these animals (Figures 3f, lower panel). These findings suggest that inhibition of GD3S does not compromise the seeding of cells to the lung but that it prevents the expansion of solitary disseminated tumor cells to macrometastatic lesions. Collectively, these data suggest that GD3S plays an important role in regulating experimental metastasis.

In order to examine the role of GD3S in EMT *in vivo*, 4T1 tumor samples were processed for histology and immunostaining with GD2 as well as EMT markers (E-cadherin and vimentin). Using H & E staining, we showed that inhibition of GD3S limits the invasion of the tumor into the surrounding tissue rendering the tumor smooth at its edges with a histology characteristic of a non-invasive tumor (Supplementary Figure 2e). GD2 was increased at the invasive front of vehicle-treated tumors whereas its expression was significantly reduced in triptolide-treated samples (Figure 3g). E-cadherin was localized mostly to the membrane in triptolide-treated tumors (Figure 3h), whereas staining was diffuse in vehicle-treated tumors. Conversely, vimentin expression was reduced (Figure 3i) in triptolide-treated 4T1 tumors compared to vehicle-treated samples. We also cultured MDA-MB-231 cells in 3D lrECM and exposed them to vehicle or triptolide. Acini were stained with laminin V as well as E-cadherin and N-cadherin. Inhibition of GD3S using triptolide inhibited N-cadherin expression (Supplementary Figure 2f, upper panel) whereas it induced laminin V and E-cadherin (Supplementary Figure 2f, lower panel). Collectively these data show that inhibition of GD3S inhibits EMT *in vitro* and *in vivo*.

GD3S expression is regulated by NF-kB via FOXC2 and predicts poor clinical outcome

Since the transcription factor FOXC2 is a downstream mediator of multiple different EMT signaling pathways,(37) we investigated whether FOXC2 could regulate GD3S expression. For this, we silenced FOXC2 expression in MDA-MB-231 and HMLE-Snail cells using shRNA and analyzed GD3S expression. We observed a significant reduction in GD3S mRNA, as well as GD3S protein, following silencing of FOXC2 in HMLE-Snail and MDA-MB-231 cells (Figures 4a-c). To examine whether FOXC2 directly regulates GD3S expression, we performed a chromatin immunoprecipitation (ChIP) assay using HMLE-Snail cells and found that FOXC2 preferentially binds to a region around 1.0 kb (-1.0 kb) upstream of the GD3S transcription start site (Figure 4d), thus confirming that GD3S is transcriptionally regulated by FOXC2. Consistent with this, using an *in vitro* wound healing assay, we observed concomitant induction of both FOXC2 and GD3S at the wound site (Supplementary Figure 2g). Since, triptolide is known to inhibit GD3S, as well as NF-kB, (38) and NF-kB is known to regulate FOXC2,(39) we examined whether NF-kB could regulate GD3S via FOXC2. For this, we overexpressed an IkB super-repressor mutant (IKB-SR), known to inhibit NF-kB, in MDA-MB-231 and HMLE-Snail cells and found that the transcripts encoding GD3S and FOXC2 were reduced following overexpression of IKB-SR (Figures 4e and f). Furthermore, overexpression of FOXC2 in these IKB-SR expressing cells restored the expression of GD3S (Figures 4g, h). To further confirm that NF-kB and FOXC2 promote EMT in a GD3S-dependent manner, we overexpressed FOXC2 in GD3S-silenced MDA-MB-231 cells and found that FOXC2 overexpression was not able to rescue either the EMT phenotype (Figure 4i) or mammosphere formation (Figure 4j) in the absence of GD3S. We also observed that overexpression of FOXC2 in MDA-MB-231 cells made them resistant to triptolide (Supplementary Figures 3a-e). Collectively, these findings indicate that GD3S expression is regulated by NF-kB via FOXC2. Moreover, our bioinformatic analyses indicate that GD3S expression is high in claudin-low/TNBCs (Figure 4k) and that it correlates with poor patient survival (Figure 4l).

GD3S regulates EMT and metastasis via activation of the c-Met signaling pathway

A recent study demonstrated that GD3S could enhance the proliferation and primary tumor growth of MDA-MB-231 cells via c-Met-signaling.(28) In order to test whether GD3S expression correlates with the active and phosphorylatable form of c-Met, we analyzed the expression of phosphorylated c-Met across a panel of cell lines that have undergone EMT or exist in a mesenchymal state. Interestingly, we observed elevated phospho-c-Met (p-c-Met) in cells with EMT/CSC properties (MDA-MB-231, SUM159, HMLE-Twist, -Snail, and -TGF-β1) relative to their epithelial counterparts (MCF-10A, HMLE-vector) even though all the cells expressed similar levels of total c-Met (Figure 5a). Moreover, the pattern of c-Met phosphorylation strongly correlates with GD3S expression in all of the cells examined (Figure 5a). To investigate if GD3S expression is regulated by c-Met, we treated the cells expressing high GD3S and p-c-Met with SU11274, a c-Met inhibitor, and found that SU11274 is capable of reducing the expression of vimentin and increasing E-cadherin levels in MDA-MB-231 cells (Figure 5b). Furthermore, SU11274 treatment substantially altered cell morphology causing increased clustering of cells into epithelial-like islands with prominent cell-cell contacts and reduced fibroblastic morphology (Figure 5c). Lastly, the

sphere-forming capacity of these cells was also significantly reduced in the presence of SU11274 (Figure 5d and Supplementary Figure 3f). While we observed loss of EMT/CSC functions in the presence of SU11274, we did not see any change in the expression of GD3S (Figure 5b) suggesting that c-Met signaling functions downstream of GD3S.

To investigate whether GD3S regulates the activation of c-Met, we examined the presence of total-c-Met as well as p-c-Met in MDA-MB-231 cells expressing GD3S-shRNA compared to the control-shRNA. Indeed, we found no change in total c-Met protein, but a significant decrease in active p-c-Met protein as well as its downstream signal mediator phospho-Akt (Figure 5e) suggesting that GD3S regulates only the function of c-Met and not its expression.

To further examine if activation of c-Met is sufficient to rescue the EMT/CSC properties in the absence of GD3S, we ectopically expressed a constitutively active form of c-Met (Tpr-Met)(29) in MDA-MB-231-shGD3S cells. Expression of Tpr-Met successfully restored the mesenchymal properties of these cells, even in the absence of GD3S, as evidenced by the acquisition of a mesenchymal-like morphology (Figure 5f), elevated expression of vimentin (Figure 5g) and enhanced mammosphere-forming efficiency relative to the control vector-expressing cells (Figure 5h). Next, we tested these cells for their ability to seed metastasis *in vivo* and found that mice injected with MDA-MB-231-shGD3S-Tpr-Met cells had significantly more lung metastases and reduced event-free survival compared to mice injected with MDA-MB-231-shGD3S-vector control cells (Figure 5i).

DISCUSSION

Recent studies have clearly shown that the EMT process can promote the generation of CSCs,(19) which contribute to therapy resistance, tumor relapse and metastasis.(17, 18, 21, 22) To achieve an optimal clinical outcome, it is imperative: 1) to identify and target cancer cells with EMT/CSC properties, preexisting within a tumor, and 2) to prevent the *de novo* generation of CSCs via EMT during therapy. In this study, we report that GD3S is expressed at high levels in claudin-low/TNBC cell lines and patient tumors and that it is necessary for the acquisition and maintenance of EMT/CSC properties in multiple EMT models and claudin-low/triple negative breast cancer cell lines. Furthermore, we demonstrate that inhibiting GD3S using shRNA or the small molecule inhibitor triptolide could provide an effective strategy for the inhibition or reversal of the mesenchymal phenotype as well as metastasis in breast cancer.

Although GD2 synthase (GD2S) is directly responsible for GD2 biosynthesis, we previously found that GD3S, and not GD2S, is the rate-limiting enzyme in GD2 biosynthesis in cells that have undergone EMT as well as in mesenchymal-looking established breast cancer cell lines.(24) Moreover, the results presented here, along with our earlier findings,(24) clearly show that GD3S is functionally important both for mesenchymal properties as well as stem cell function. Although, it is not clear how an enzyme involved in GD2 biosynthesis might regulate EMT, migration, invasion and metastasis, we speculate that GD2—the product of the GD3S biosynthetic pathway—may play a pivotal role in regulating these attributes either in an inter- or intra-cellular manner. Furthermore, we have established links between GD3S

expression and activation of the c-Met signaling pathway. Moreover, our findings demonstrate that GD3S is important for the initiation of EMT in response to TGF-β1 as well as Snail and Twist. In addition, we have shown that NF-kB—known to respond to numerous inflammatory stimuli—can indirectly regulate GD3S transcription via the transcription factor FOXC2, a central mediator of multiple EMT programs. Thus, we speculate that GD3S may possibly play an important role in regulating EMT properties in response to a variety of EMT-promoting signals emanating from the tumor microenvironment including TNF-alpha. With these considerations in mind, we propose that GD3S is likely to be an important therapeutic target for multiple EMT pathways operating in breast tumors.

Whereas inhibition of GD3S, using shRNA or triptolide, significantly reduced the metastatic burden in mice, it also reduced primary tumor growth. This suggests that GD3S and, possibly GD2, may be important for the expansion of tumor cells *in vivo* but not *in vitro*, because inhibition of GD3S did not affect cell proliferation rates *in vitro*. This is further evidenced upon closer examination of the lungs in the mice injected with GD3S shRNA-expressing cells or treated with triptolide, in which we observed numerous presumably dormant solitary tumor cells that failed to grow into macroscopic nodules. These data suggest that GD3S is important for the differentiation/expansion of cells after they have seeded to the lung. Indeed, this fits well with our data that inhibition of GD3S inhibits c-Met signaling, which is important for the sustained proliferation and self-renewal properties of CSCs.(40

Our data indicate that GD3S expression is high in TNBCs and that its expression predicts poor clinical outcome, consistent with the notion that GD3S-mediated generation of GD2 enhances stem cell properties and may be responsible for the aggressive nature of these tumors and the poor clinical outcome observed. Since GD3S is an enzyme and there is a small molecule inhibitor available to inhibit its expression, we believe that our data attest to the potential efficacy of triptolide for the treatment of TNBCs and for eradicating CSC-enriched tumors. Our findings also suggest that targeting GD3S or c-Met signaling could be effective against tumor progression and metastasis. The findings presented here establish GD3S as a novel functional gene specific to cells that have undergone EMT as well as mesenchymal-looking breast cancer cells and suggest that GD3S could serve as a novel therapeutic target for mesenchymal-appearing triple negative claudin-low tumors. Since targeted agents against GD3S, e.g. triptolide,(41) are currently in clinical trials, we envisage that the optimal clinical outcome will only be achieved by using triptolide or c-Met inhibitor to eradicate CSCs in combination with standard-of-care therapies that target the differentiated cells of the tumor bulk and that this approach will be effective for treating primary tumors and metastases.

MATERIALS AND METHODS

Cells and culture conditions

Immortalized human mammary epithelial cells (HMLE) and cells expressing empty vector (pWZL), Snail, Twist, or an activated form of TGF-β1 were maintained as previously described. (10, 19, 37) Breast cancer cell lines SUM159 and MDA-MB-231 were cultured as described in Hollier *et al*.(37) For assays characterizing the resistance of cells to cytotoxic

compounds, cells were seeded at a density of 8×10^3 cells per well of 96-well plates. After 24 h, medium was replaced with fresh growth medium (100 μl/well) containing the indicated concentrations of triptolide dissolved in DMSO. Control cells were treated with DMSO. Cell viability was assessed using the CellTiter96 Aqueous One Solution Cell Proliferation Assay (Promega, Madison, WI, USA). The mouse mammary tumor 4T1 cells were cultured as described.(10)

Plasmids and viral transduction

The method used for the production of lentiviruses and amphotropic retroviruses as well as the transduction of target cells was previously described.(42) IKB SR puromycin resistant construct was a gift from Dr. Weston Porter (Texas A & M University). Tpr-Met overexpressing cells were generated by retroviral transduction of cells with a pWZL-Blast construct encoding the cDNA for Tpr-Met and selection in 4 μg/ml of blasticidin (Invitrogen).

Antibodies, western blotting and immunofluorescence

For western blotting, proteins were extracted by lysing cells in ice-cold radio-immunoprecipitation (RIPA) buffer containing protease and phosphatase inhibitors (Roche, Nutley, NJ, USA). Protein was quantified using the Bradford Assay (BioRad, Hercules, CA, USA) and 50 μg of total protein was resolved using 4-12% Bis-Tris SDS-PAGE gels (NuPage, Invitrogen) and transferred to PVDF membranes. Membranes were probed with primary antibodies, including anti-β-actin (Sigma A3853, St. Louis, MO, USA), FOXC2 (developed by Dr. Naoyuki Miura, Hamamatsu University School of Medicine, Japan), E-cadherin (BD, 61081, San Jose, CA, USA), fibronectin (BD, 610077), N-cadherin (BD, 610910), vimentin (Novus, NB200-623, Littleton, CO, USA), GD3 synthase (Abcam, Ab37806, Cambridge, England, SCBT, Dallas, Texas, USA, sc-99093), c-Met (Cell signaling, Danvers, CA, USA, 3127S), p-c-Met (Cell Signaling, 3077P), p-Smad (Santa Cruz, sc-11769-R), Smad (Santa Cruz, sc-6032), p-Akt (Cell signaling, 9271S), Akt (Cell signaling, 9272). Following incubation with horseradish peroxidase-conjugated secondary species-specific antibodies, immunoreactive proteins were detected using chemiluminescence (ECL Plus, GE Healthcare, Barrington, IL). Immunofluorescence staining of cells was performed as previously described (37) and formalin-fixed paraffin-embedded tissue sections were stained as described(43) using the above mentioned antibodies along with GD2 (BD, clone 14G2a).

Cell culture assays and ChIP

Fluorescence-activated cell sorting (FACS)(24), Chromatin immunoprecipitation (37), Three-dimensional (3D) laminin-rich extracellular matrix (lrECM) on-top cultures (36, 37) and mammosphere assays (19) were conducted as previously described.

Animal studies

NOD/SCID and BALB/C mice were purchased from the Jackson Laboratory (Maine, USA) and all mouse procedures were approved by the Animal Care and Use Committees of the University of Texas MD Anderson Cancer Center and performed in accordance with

Institutional policies. To assess the experimental metastatic potential of cells, 5×10^5 MDA-MB-231- control-shRNA and GD3S shRNA cells labeled with RFP-firefly luciferase were injected into NOD/SCID mice via the tail vein. Mice were assessed weekly for metastasis via the intraperitoneal injection of D-Luciferin (Caliper LifeSciences). After allowing 10 minutes, *in vivo* bioluminescence was assessed using the IVIS imaging system 200 series (Xenogen Corporation). Mice were monitored for lung metastasis and sacrificed after 6 weeks, at which time the lungs were surgically removed and fixed using Bouin's fluid and the number of lung tumor nodules was counted using a dissection microscope. Lungs were further subjected to H & E staining and stained for RFP to ascertain the presence of MDA-MB-231 cells. To assess the inhibitory effect of triptolide on experimental metastasis, 0.5×10^6 MDA-MB-231 cells labeled with RFP-firefly luciferase were injected into NOD/SCID mice via tail vein injection. Thereafter, triptolide (0.15 mg/kg/day) was administered intraperitoneally on a daily basis. Mice were sacrificed after 6 weeks, and lung metastatic nodules were quantified as detailed above.

To examine the role of GD3S on tumor formation and spontaneous metastasis, 0.1×10^6 4T1-control-shRNA and 4T1-GD3S shRNA cells were injected orthotopically into the mammary fat pad of BALB/c mice. Mice were assessed weekly for tumor size and metastasis via the intraperitoneal injection of D-Luciferin. Tumors and lung metastases were measured after sacrificing the mice at 3 weeks. To confirm the role of GD3S on the progression of metastasis, 10,000 4T1 cells were injected into BALB/c mice and once palpable tumors had formed, one set of mice was treated with triptolide and the other set was treated with vehicle. Tumors and lung metastases were measured after sacrificing the mice at 5 weeks. To ascertain the role of Tpr-Met on experimental metastasis in the absence of GD3S, 0.5×10^6 MDA-MB-231-GD3S shRNA-vector and MDA-MB-231-GD3S shRNA-Tpr-Met cells, labeled with RFP-firefly luciferase, were injected into NOD/SCID mice via tail vein injection. Mice were assessed weekly for metastasis via the intraperitoneal injection of D-Luciferin. The Kaplan-Meier survival curve was generated.

Quantitative reverse transcription PCR (qRT-PCR

Total RNA was isolated using the RNeasy Plus kit (Qiagen) according to the manufacturer's instructions. All qRT-PCR experiments were run in triplicate and a mean value was used for the determination of mRNA levels. Relative quantification of the mRNA levels was performed using the comparative Ct method with GAPDH as the reference gene and with the formula $2^{-\Delta\Delta Ct}$.

Scratch assays

Cells (approximately 3×10^5 cells/well) were seeded in culture dishes and allowed to adhere for 8 to 10 h in medium containing 0.5% FBS in the case of MDA-MB-231 and only medium without FBS in the case of HMLE-Snail cells. A scratch was done using a sterile pipette tip and the dish was filled with fresh medium. Wound closure was monitored and recorded over time.

Supplementary Material

Refer to Web version on PubMed Central for supplementary material.

ACKNOWLEDGEMENTS

The authors acknowledge the entire Mani Lab for invaluable suggestions and discussions. We acknowledge Thiru Arumugam for his valuable help in animal imaging. This work was supported by an MD Anderson Research Trust Fellow Award, funded by the George and Barbara Bush Endowment for Innovative Cancer Research (SAM). Flow cytometry, confocal microscopy, and animal imaging were in part funded by the Cancer Center Support Grant from the National Cancer Institute (CA16672). The authors also acknowledge support from the Breast Cancer Research Foundation (to MA) and the Rolanette and Berdon Lawrence Research award from Bone Disease Program of Texas (to VLB).

REFERENCES

1. Hay ED. An overview of epithelio-mesenchymal transformation. Acta Anat (Basel). 1995; 154:8–20. [PubMed: 8714286]
2. Thiery JP, Acloque H, Huang RY, Nieto MA. Epithelial-mesenchymal transitions in development and disease. Cell. 2009; 139:871–890. [PubMed: 19945376]
3. Haynes J, Srivastava J, Madson N, Wittmann T, Barber DL. Dynamic actin remodeling during epithelial-mesenchymal transition depends on increased moesin expression. Mol Biol Cell. 2011; 22:4750–4764. [PubMed: 22031288]
4. Kiemer AK, Takeuchi K, Quinlan MP. Identification of genes involved in epithelial-mesenchymal transition and tumor progression. Oncogene. 2001; 20:6679–6688. [PubMed: 11709702]
5. Vincent-Salomon A, Thiery JP. Host microenvironment in breast cancer development: epithelial-mesenchymal transition in breast cancer development. Breast Cancer Res. 2003; 5:101–106. [PubMed: 12631389]
6. Xue C, Plieth D, Venkov C, Xu C, Neilson EG. The gatekeeper effect of epithelial-mesenchymal transition regulates the frequency of breast cancer metastasis. Cancer Res. 2003; 63:3386–3394. [PubMed: 12810675]
7. Janda E, Lehmann K, Killisch I, Jechlinger M, Herzig M, Downward J, et al. Ras and TGF[beta] cooperatively regulate epithelial cell plasticity and metastasis: dissection of Ras signaling pathways. J Cell Biol. 2002; 156:299–313. [PubMed: 11790801]
8. Oft M, Peli J, Rudaz C, Schwarz H, Beug H, Reichmann E. TGF-beta1 and Ha-Ras collaborate in modulating the phenotypic plasticity and invasiveness of epithelial tumor cells. Genes Dev. 1996; 10:2462–2477. [PubMed: 8843198]
9. Birchmeier C, Birchmeier W, Gherardi E, Vande Woude GF. Met, metastasis, motility and more. Nat Rev Mol Cell Biol. 2003; 4:915–925. [PubMed: 14685170]
10. Yang J, Mani SA, Donaher JL, Ramaswamy S, Itzykson RA, Come C, et al. Twist, a master regulator of morphogenesis, plays an essential role in tumor metastasis. Cell. 2004; 117:927–939. [PubMed: 15210113]
11. Cano A, Perez-Moreno MA, Rodrigo I, Locascio A, Blanco MJ, del Barrio MG, et al. The transcription factor snail controls epithelial-mesenchymal transitions by repressing E-cadherin expression. Nat Cell Biol. 2000; 2:76–83. [PubMed: 10655586]
12. Hartwell KA, Muir B, Reinhardt F, Carpenter AE, Sgroi DC, Weinberg RA. The Spemann organizer gene, Goosecoid, promotes tumor metastasis. Proc Natl Acad Sci U S A. 2006; 103:18969–18974. [PubMed: 17142318]
13. Onder TT, Gupta PB, Mani SA, Yang J, Lander ES, Weinberg RA. Loss of E-cadherin promotes metastasis via multiple downstream transcriptional pathways. Cancer Res. 2008; 68:3645–3654. [PubMed: 18483246]
14. Huber MA, Kraut N, Beug H. Molecular requirements for epithelial-mesenchymal transition during tumor progression. Curr Opin Cell Biol. 2005; 17:548–558. [PubMed: 16098727]

15. Zavadil J, Cermak L, Soto-Nieves N, Bottinger EP. Integration of TGF-beta/Smad and Jagged1/Notch signalling in epithelial-to-mesenchymal transition. EMBO J. 2004; 23:1155–1165. [PubMed: 14976548]
16. Bates RC, Mercurio AM. Tumor necrosis factor-alpha stimulates the epithelial-to-mesenchymal transition of human colonic organoids. Mol Biol Cell. 2003; 14:1790–1800. [PubMed: 12802055]
17. Fillmore CM, Kuperwasser C. Human breast cancer cell lines contain stem-like cells that self-renew, give rise to phenotypically diverse progeny and survive chemotherapy. Breast Cancer Res. 2008; 10:R25. [PubMed: 18366788]
18. Gupta PB, Onder TT, Jiang G, Tao K, Kuperwasser C, Weinberg RA, et al. Identification of selective inhibitors of cancer stem cells by high-throughput screening. Cell. 2009; 138:645–659. [PubMed: 19682730]
19. Mani SA, Guo W, Liao MJ, Eaton EN, Ayyanan A, Zhou AY, et al. The epithelial-mesenchymal transition generates cells with properties of stem cells. Cell. 2008; 133:704–715. [PubMed: 18485877]
20. Morel AP, Lievre M, Thomas C, Hinkal G, Ansieau S, Puisieux A. Generation of breast cancer stem cells through epithelial-mesenchymal transition. PLoS One. 2008; 3:e2888. [PubMed: 18682804]
21. Li X, Lewis MT, Huang J, Gutierrez C, Osborne CK, Wu MF, et al. Intrinsic resistance of tumorigenic breast cancer cells to chemotherapy. J Natl Cancer Inst. 2008; 100:672–679. [PubMed: 18445819]
22. Creighton CJ, Li X, Landis M, Dixon JM, Neumeister VM, Sjolund A, et al. Residual breast cancers after conventional therapy display mesenchymal as well as tumor-initiating features. Proc Natl Acad Sci U S A. 2009; 106:13820–13825. [PubMed: 19666588]
23. Battula VL, Evans KW, Hollier BG, Shi Y, Marini FC, Ayyanan A, et al. Epithelial-mesenchymal transition-derived cells exhibit multilineage differentiation potential similar to mesenchymal stem cells. Stem Cells. 2010; 28:1435–1445. [PubMed: 20572012]
24. Battula VL, Shi Y, Evans KW, Wang RY, Spaeth EL, Jacamo RO, et al. Ganglioside GD2 identifies breast cancer stem cells and promotes tumorigenesis. J Clin Invest. 2012; 122:2066–2078. [PubMed: 22585577]
25. Schmidt C, Bladt F, Goedecke S, Brinkmann V, Zschiesche W, Sharpe M, et al. Scatter factor/hepatocyte growth factor is essential for liver development. Nature. 1995; 373:699–702. [PubMed: 7854452]
26. Bladt F, Riethmacher D, Isenmann S, Aguzzi A, Birchmeier C. Essential role for the c-met receptor in the migration of myogenic precursor cells into the limb bud. Nature. 1995; 376:768–771. [PubMed: 7651534]
27. Zhang YW, Vande Woude GF. HGF/SF-met signaling in the control of branching morphogenesis and invasion. J Cell Biochem. 2003; 88:408–417. [PubMed: 12520544]
28. van Leenders GJ, Sookhlall R, Teubel WJ, de Ridder CM, Reneman S, Sacchetti A, et al. Activation of c-MET induces a stem-like phenotype in human prostate cancer. PLoS One. 2011; 6:e26753. [PubMed: 22110593]
29. Ma PC, Tretiakova MS, Nallasura V, Jagadeeswaran R, Husain AN, Salgia R. Downstream signalling and specific inhibition of c-MET/HGF pathway in small cell lung cancer: implications for tumour invasion. Br J Cancer. 2007; 97:368–377. [PubMed: 17667909]
30. Di Renzo MF, Poulsom R, Olivero M, Comoglio PM, Lemoine NR. Expression of the Met/hepatocyte growth factor receptor in human pancreatic cancer. Cancer Res. 1995; 55:1129–1138. [PubMed: 7866999]
31. Tsao MS, Liu N, Chen JR, Pappas J, Ho J, To C, et al. Differential expression of Met/hepatocyte growth factor receptor in subtypes of non-small cell lung cancers. Lung Cancer. 1998; 20:1–16. [PubMed: 9699182]
32. Schmidt L, Duh FM, Chen F, Kishida T, Glenn G, Choyke P, et al. Germline and somatic mutations in the tyrosine kinase domain of the MET proto-oncogene in papillary renal carcinomas. Nat Genet. 1997; 16:68–73. [PubMed: 9140397]
33. Tuck AB, Park M, Sterns EE, Boag A, Elliott BE. Coexpression of hepatocyte growth factor and receptor (Met) in human breast carcinoma. Am J Pathol. 1996; 148:225–232. [PubMed: 8546209]

34. Cazet A, Lefebvre J, Adriaenssens E, Julien S, Bobowski M, Grigoriadis A, et al. GD(3) synthase expression enhances proliferation and tumor growth of MDA-MB-231 breast cancer cells through c-Met activation. Mol Cancer Res. 2010; 8:1526–1535. [PubMed: 20889649]

35. Kwon HY, Kim SJ, Kim CH, Son SW, Kim KS, Lee JH, et al. Triptolide downregulates human GD3 synthase (hST8Sia I) gene expression in SK-MEL-2 human melanoma cells. Exp Mol Med. 2010; 42:849–855. [PubMed: 21072003]

36. Debnath J, Muthuswamy SK, Brugge JS. Morphogenesis and oncogenesis of MCF-10A mammary epithelial acini grown in three-dimensional basement membrane cultures. Methods. 2003; 30:256–268. [PubMed: 12798140]

37. Hollier BG, Tinnirello AA, Werden SJ, Evans KW, Taube JH, Sarkar TR, et al. FOXC2 expression links epithelial-mesenchymal transition and stem cell properties in breast cancer. Cancer Res. 2013; 73:1981–1992. [PubMed: 23378344]

38. Hao L, Zhi-Hong L, Zhao-Hong C, Jun-Wei Y, Lei-Shi L. Triptolide a potent inhibitor of NF-kB in T lymphocytes. Acta Pharmacol Sin. 2000; 21:782–786. [PubMed: 11501157]

39. Yu YH, Chen HA, Chen PS, Cheng YJ, Hsu WH, Chang YW, et al. MiR-520h-mediated FOXC2 regulation is critical for inhibition of lung cancer progression by resveratrol. Oncogene. 2013; 32:431–443. [PubMed: 22410781]

40. Li YLA, Glas M, Lal B, Ying M, Sang Y, Xia S, Trageser D, Guerrero-Cázares H, Eberhart CG, Quiñones-Hinojosa A, Scheffler B, Laterra J. c-Met signaling induces a reprogramming network and supports the glioblastoma stem-like phenotype. Proc Natl Acad Sci U S A. 2011; 108:9951–9956. [PubMed: 21628563]

41. Kiviharju TM, Lecane PS, Sellers RG, Peehl DM. Antiproliferative and proapoptotic activities of triptolide (PG490), a natural product entering clinical trials, on primary cultures of human prostatic epithelial cells. Clin Cancer Res. 2002; 8:2666–2674. [PubMed: 12171899]

42. Stewart SA, Dykxhoorn DM, Palliser D, Mizuno H, Yu EY, An DS, et al. Lentivirus-delivered stable gene silencing by RNAi in primary cells. RNA. 2003; 9:493–501. [PubMed: 12649500]

43. Guo W, Keckesova Z, Donaher JL, Shibue T, Tischler V, Reinhardt F, et al. Slug and Sox9 cooperatively determine the mammary stem cell state. Cell. 2012; 148:1015–1028. [PubMed: 22385965]

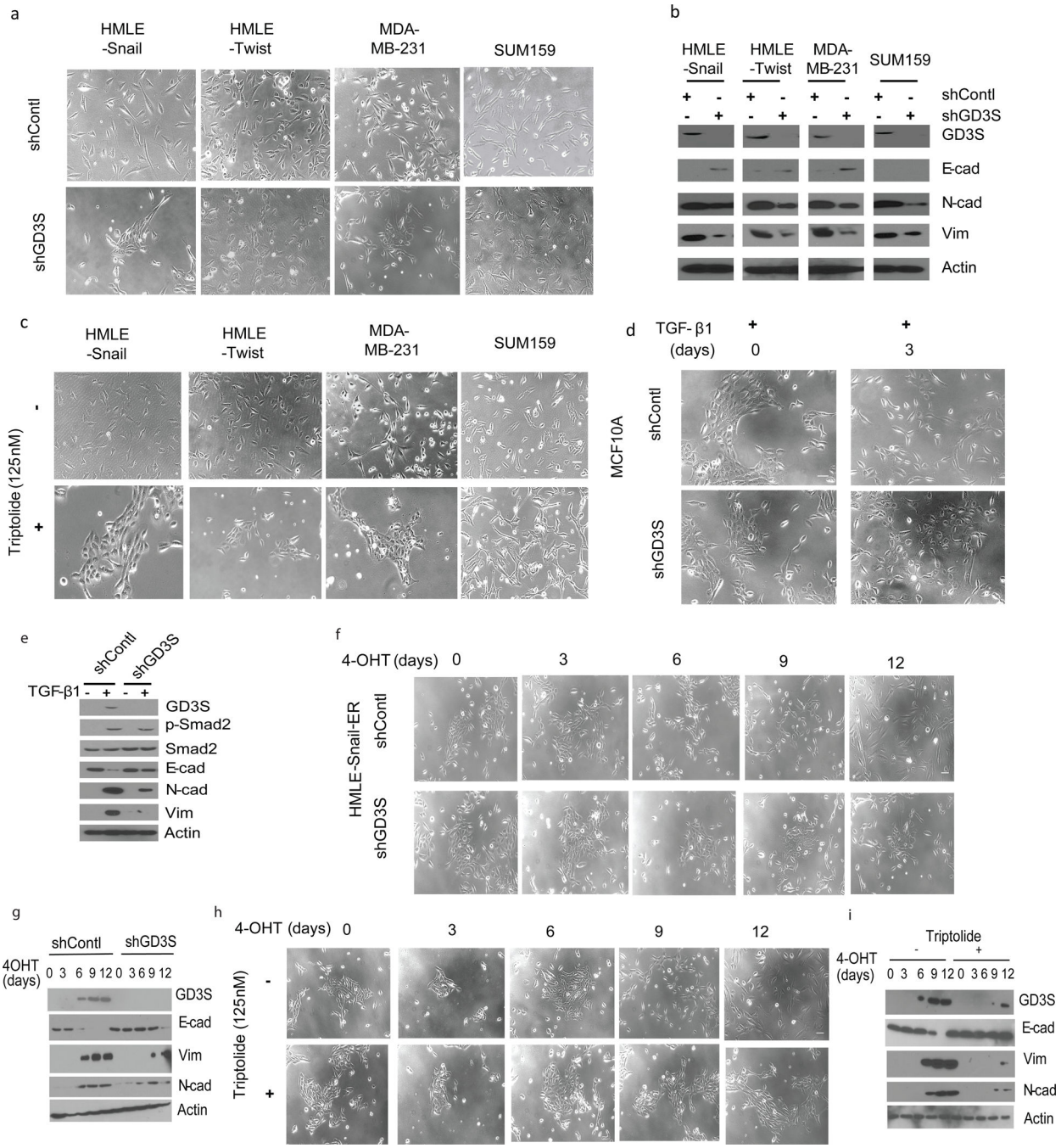

Figure 1. GD3S plays an important role in the initiation and maintenance of EMT

(a-c) GD3S was inhibited in the studied cell lines either by shRNA-mediated silencing (a) or by treating the cells with triptolide (c) and the phenotype was examined along with western analysis for epithelial and mesenchymal markers (b). Morphological analysis (d) as well as western analysis (e) of TGF-β1 treated MCF-10A cells in the presence or absence of GD3S. (f-i) Morphology (f, h) and western analysis (g, i) of tamoxifen-treated HMLE-Snail-ER cells after inhibition of GD3S by either shRNA (f, g) or triptolide (h, i).

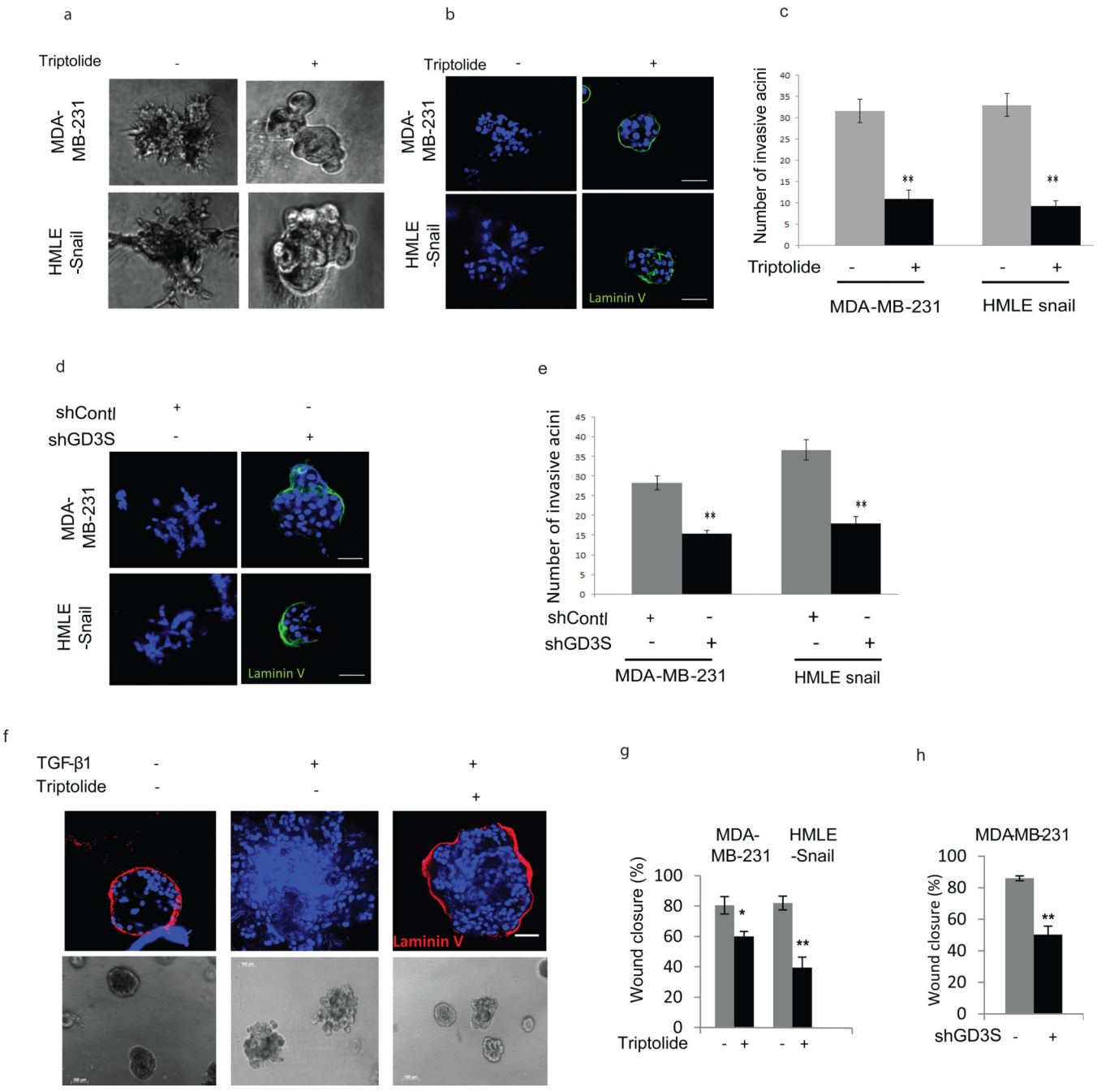

Figure 2. Inhibition of GD3S inhibits invasion and motility of cancer cells

(a-e) Control-shRNA, GD3S-shRNA (a, b), vehicle and triptolide-treated (a, b, c) MDA-MB-231 and HMLE-Snail cells were grown on matrigel and the formation of 3-dimensional spheroid acinus structures was observed and quantified after 10 days. Immunofluorescence was performed to ascertain the integrity of the laminin V basement membrane. (d) A scratch assay was performed using MDA-MB-231 control-shRNA, MDA-MB-231 GD3S-shRNA, vehicle- and triptolide-treated MDA-MB-231 and HMLE-Snail cells. Wound closure was measured by image analysis and represented in a graphical format. Data are represented as mean +/− SEM. P values were calculated using Student's t test. *P ≤ 0.05; **P ≤ 0.01; ***P

≤ 0.001. Scale bars, 100μm. (e) The effect of triptolide treatment on TGF-β1 mediated EMT induction in MCF10A cells was examined in 3D culture. Acini were immunostained with antibodies against the basement membrane marker laminin V (red) and counterstained with DAPI (blue) nuclear stain. Scale bars, 100μm.

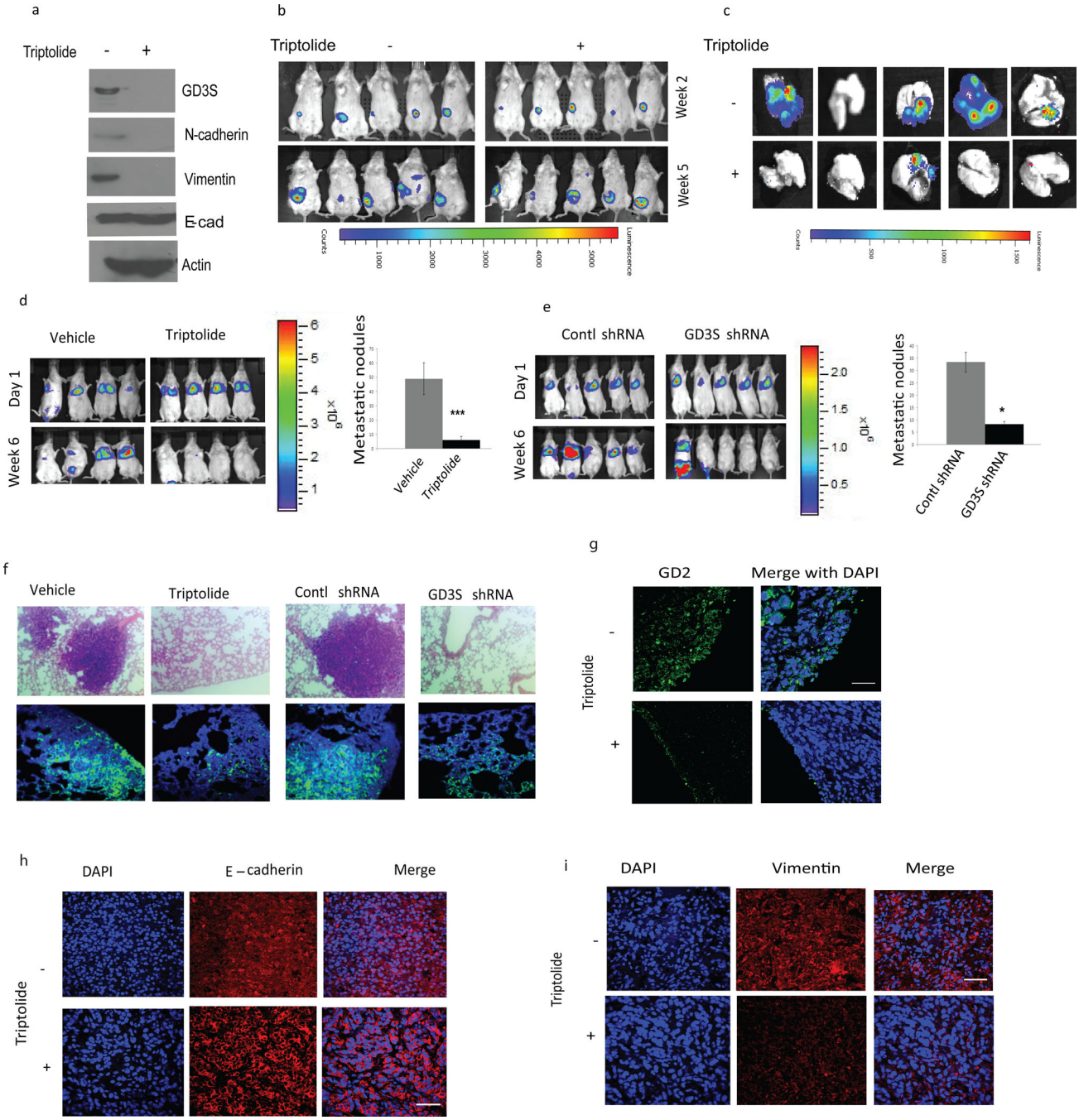

Figure 3. Inhibition of GD3S inhibits metastasis

(a-c) The effect of GD3S inhibition on metastasis in syngeneic wild-type hosts was examined. After confirming GD3S knockdown at the protein level via western blotting (a), 4T1 cells were injected into the mammary fat pad of BALB/c mice. After forming palpable tumors (b, top panel), mice were treated with either vehicle or triptolide. The incidence of metastasis was measured by luciferin injection and bioluminescence imaging. Mice were sacrificed at 5 weeks and the lung metastases were quantified by bioluminescence imaging (c). (d) MDA-MB-231 cells were injected via the tail vein and the corresponding mice were

treated with either vehicle (DMSO) or triptolide. The development of metastasis was monitored by luciferin injection and bioluminescence imaging (d, left panel). After 6 weeks, the mice were sacrificed and the lungs were surgically removed and fixed overnight in Bouin's solution and metastatic nodules were counted (d, right panel). (e) Luciferase-labeled MDA-MB-231 control-shRNA and GD3S-shRNA cells were introduced into mice via tail vein injection and the development of metastasis was monitored by luciferin injection and bioluminescence imaging. After 6 weeks, the mice were sacrificed and the lungs were surgically removed, fixed overnight in Bouin's solution and metastatic nodules were counted. (f) H & E staining of the lungs from mice injected with MDA-MB-231 cells and subsequently treated with vehicle or triptolide (upper left panel). H & E staining of the lungs from mice injected with MDA-MB-231 control-shRNA and GD3S-shRNA cells (f, upper right panel). Lungs were immunostained with anti-RFP antibody to examine the colonizing efficiency of MDA-MB-231 cells in the lungs following inhibition of GD3S either by triptolide (f, lower left panel) or by GD3S-shRNA (f, lower right panel). Data are represented as mean +/− SEM. P values were calculated using Student's t test. *$P \leq 0.05$; **$P \leq 0.01$; ***$P \leq 0.001$. (g) 4T1 tumors were immunostained with anti-GD2 antibody to observe the pattern of GD2 expression in the absence or presence of triptolide. (h, i) 4T1 tumors were immunostained with EMT markers such as E-cadherin (h) or vimentin (i) in order to examine the effect of triptolide on EMT markers *in vivo*.

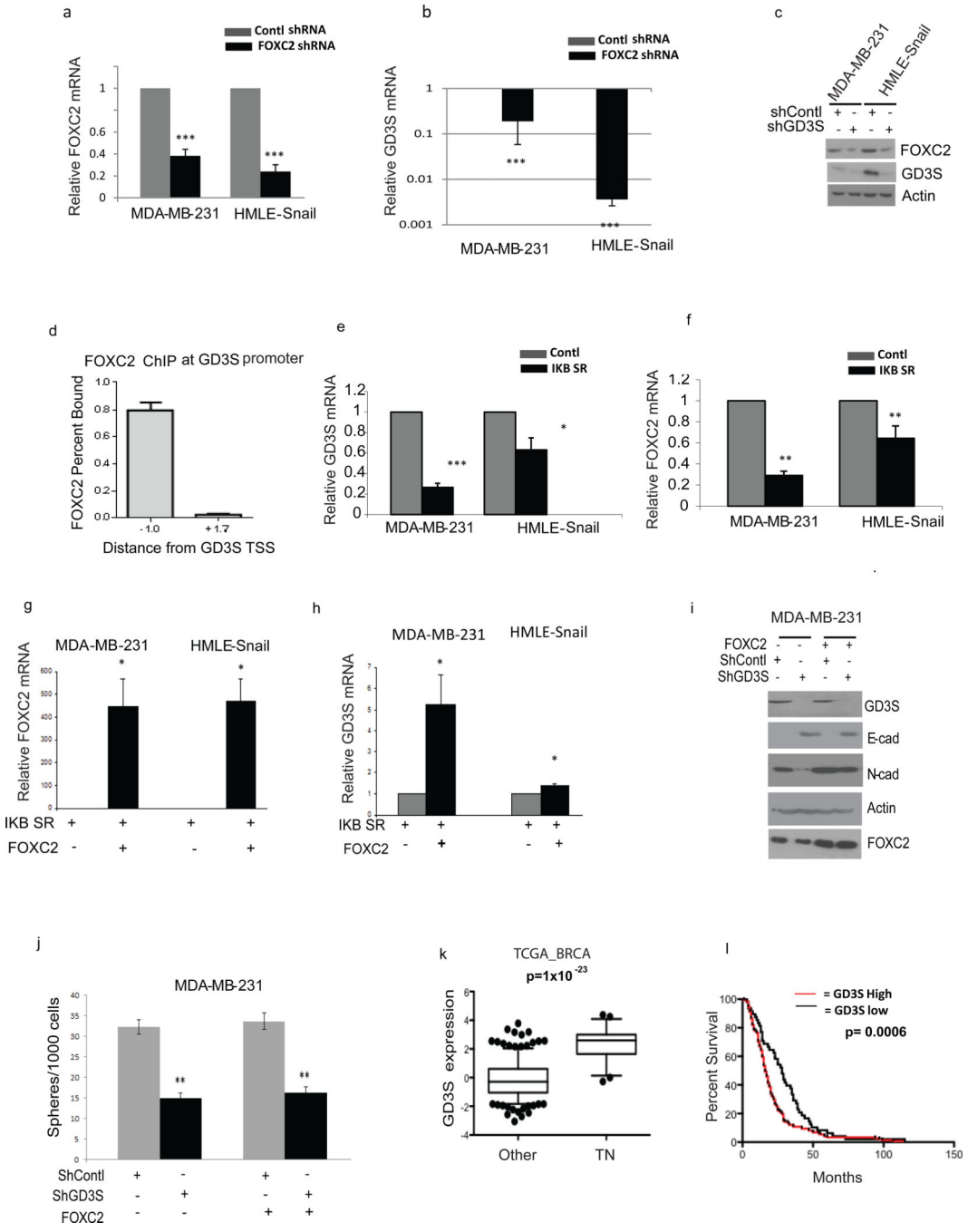

Figure 4. NF-kB regulates GD3S via FOXC2

(a-c) FOXC2 was silenced in MDA-MB-231 and HMLE-Snail cells (a), and GD3S transcript (b) and protein levels (c) were measured. (d) A chromatin immunoprecipitation assay was performed using MDA-MB-231 cells to show that the FOXC2 protein binds to the promoter region of GD3S. The X axis denotes distance from the transcription start site in kb. (e, f) MDA-MB-231 and HMLE-Snail cells were transfected with IKB SR and the transcript levels of GD3S (e) and FOXC2 (f) were analyzed by qRT-PCR. (g, h) FOXC2 was overexpressed in IKB SR transduced MDA-MB-231 and HMLE-Snail cells and the

transcript levels of FOXC2 (g) and GD3S (h) were analyzed by qRT-PCR. FOXC2 was overexpressed in MDA-MB-231 cells in the presence of either control-shRNA or GD3S shRNA and the protein (i) level of FOXC2 , GD3S and EMT markers were analyzed by immunoblotting . (j) The mammosphere forming efficiency of MDA-MB-231 overexpressing FOXC2, in the presence of either control-shRNA or GD3S shRNA, was determined. (k, l) A bioinformatics study was performed using The Cancer Genome Atlas Breast Cancer database (TCGA_BRCA) to analyze the GD3S expression pattern in non-triple negative versus triple negative breast cancer patients (k) as well as to determine the correlation between GD3S overexpression and patient survival (l). TN represents triple negative breast cancers whereas OTHER represents the remainder of the breast cancers.

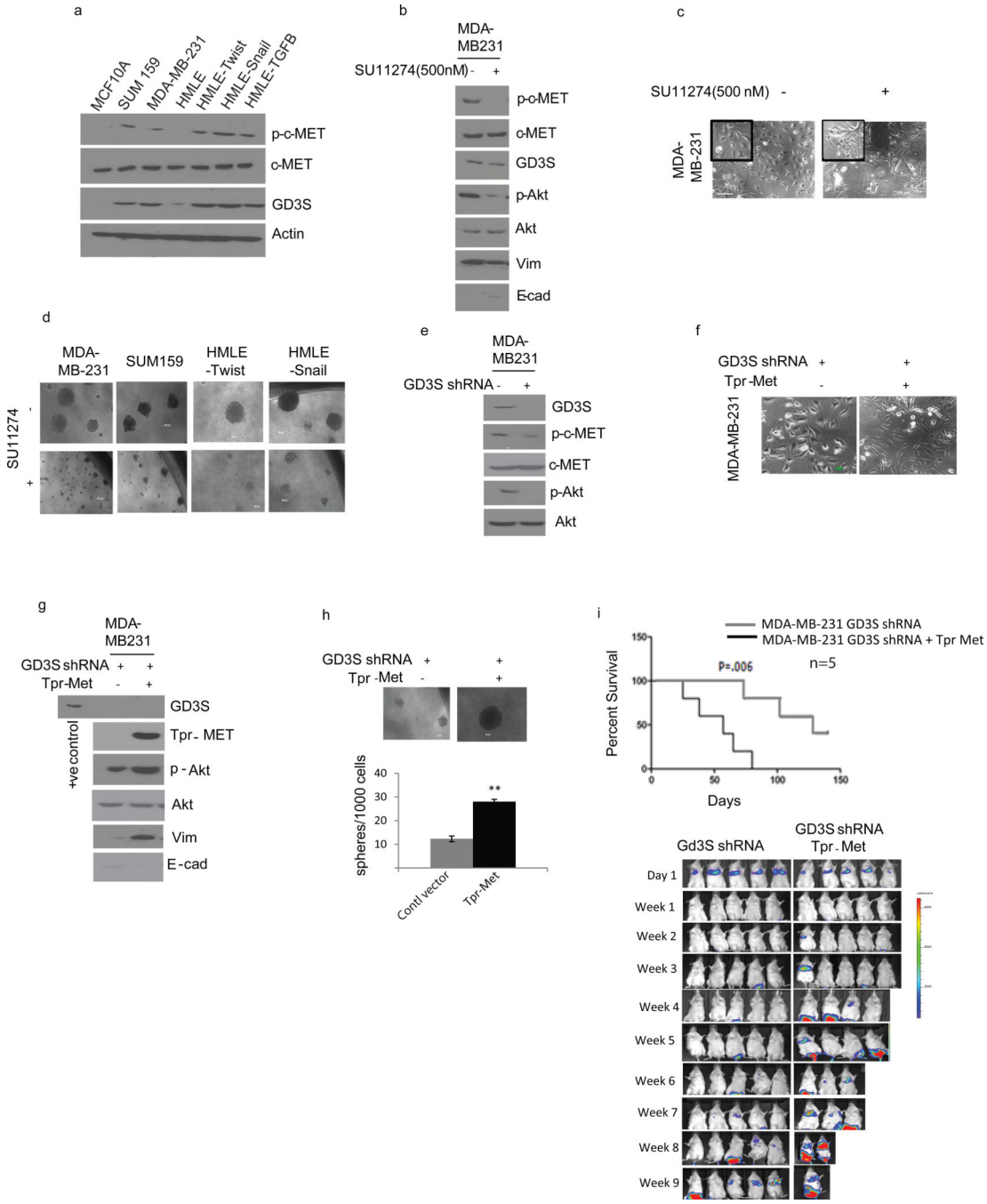

Figure 5. GD3S regulates EMT and metastasis via the HGF/c-Met signaling pathway

(a) Western analysis of p-c-Met, c-Met, GD3S and actin expression in a panel of breast cancer cells (MCF-10A, MDA-MB-231, SUM159, HMLE) and cells induced to undergo EMT by different stimuli (HMLE-Twist, HMLE-Snail, HMLE-TGF-β1). MDA-MB-231 cells were treated with SU11274 (c-MET inhibitor) and used for analysis of p-c-Met, GD3S and EMT markers (E-cadherin and vimentin) by immunoblotting (b) as well as cell morphology (c). (d). MDA-MB-231, SUM159, HMLE-Twist, and HMLE-Snail cells were treated with SU11274 and subjected to a mammosphere assay. (e) Activation of c-Met (p-c-

Met) was analyzed using control and GD3S-silenced MDA-MB-231 cells. p-Akt was used as a downstream indicator of c-Met signaling. (f) Tpr-Met was overexpressed in GD3S shRNA-transduced MDA-MB-231 cells and their respective morphologies are pictured. (g) Tpr-Met was overexpressed in MDA-MB-231 GD3S-shRNA cells and cell lysates were used to analyze EMT markers (such as E-cadherin and vimentin) as well as p-Akt. (h) Tpr-Met transduced MDA-MB-231 GD3S-shRNA cells were used for a mammosphere assay. (i) MDA-MB-231 GD3S-shRNA and Tpr-Met transduced MDA-MB-231 GD3S-shRNA cells were introduced into mice via tail vein injection. The generation of lung metastases was monitored and the Kaplan-Meier survival curves were plotted. Data are represented as mean +/− SEM. P values were calculated using Student's t test. *P ≤ 0.05; **P ≤ 0.01; ***P ≤ 0.001. Scale bars, 100μm. (j) Western analysis was performed with the whole cell lysates from control and FOXC2 shRNA transfected MDA-MB-231 cells to analyze the levels of GD3S, p-c-MET. c-MET and FOXC2.